Progress In Electromagnetics Research Letters, Vol. 102, 27–36, 2022

Dual Circularly Polarized Wideband Magneto-Electric Dipole Antenna for Wireless Applications

Xiaoxiang Ding[1, *], Shinan Wu[2], Guoqing Yang[1], and Hai Lan[1]

Abstract—A wideband magneto-electric (ME) dipole with characteristics of dual-circular polarization is presented in this paper. The proposed antenna is composed of four horizontal radiation patches, four pairs of vertical radiation patches, a ground plane, a pair of wideband feeding networks, and novel crossed feeding structures which work as wideband 3-stage impedance matching transitions. The feeding networks which contain a Wilkinson power divider and a coupled-line phase shifter are printed on the bottom of the ground plane, and they can provide stable two-way output wideband signals with quadrature-phase. The proposed antenna works as a ME dipole with a wide operation bandwidth of 53.2% ($S_{11} < -10$ dB, and Axial Ratio (AR) < 3 dB) from 1.71 GHz to 2.95 GHz for right-hand circular polarization (RHCP) and 62% from 1.7 GHz to 3.25 GHz for left-hand circular polarization (LHCP), respectively.

1. INTRODUCTION

The rapid development of wireless communications is inseparable from the upgrading of antennas, especially wideband antennas with circularly polarized (CP) characteristics. It is well known that compared with linearly polarized (LP) antennas, CP antennas show more excellent performances and have been widely used in modern wireless communication systems, such as global position systems (GPS) [1], wireless local area networks (WLANs) [2], radio frequency identification (RFID) readers [3], and satellite communications [4]. The required bandwidth of CP antennas usually should be wider than 20% to meet the needs of wideband applications. Specially, antennas with multiple polarization diversity satisfying multi-functional modes are urgently needed for channel capacity enhancement and link quality improvement. A dual-band dual-sense CP crossed dipole antenna [5] is proposed to satisfy WLAN and WiMAX's applications. Alternatively, slot antennas [6, 7] and loop antennas [8] can also achieve dual circular polarizations. Unfortunately, limited by the inherent narrowband characteristics of the radiation structures, their operation bandwidth is usually less than 10%, which makes it unable to be used in wideband systems.

A magneto-electric (ME) dipole antenna was first proposed in 2006 by Prof. Luk in [9]. Due to its wide bandwidth performance, low cross-polarization, and high gain, ME dipole antenna has been widely investigated and used in many real wireless communication situations, such as dual-wideband applications [10, 11], low-profile with substrate integration [12], and compactness with folded structures [13]. ME dipole antenna is an ideal choice to accomplish multiple polarization diversity. Therefore, some types of polarization diversity designs based on ME dipole [14, 15] have been presented. By reconfiguring the PIN diodes implanted in radiation structures or feeding networks, antennas with a single feeding port can achieve two or more polarization modes.

However, additional DC biasing circuits are required to complete the controlling of the PIN diodes, which makes antenna structures complex and introduces additional DC power consumption. Using

Received 25 November 2021, Accepted 22 December 2021, Scheduled 2 January 2022

* Corresponding author: Xiaoxiang Ding (dxx5050@163.com).

[1] Southwest Institute of Electronic Technology of China, Chengdu 610036, China. [2] School of Electronic Engineering, University of Electronic Science and Technology of China, Chengdu 611731, Sichuan, China.

two or more ports to realize multiple polarized radiations is a viable alternative option. A wideband dual-LP ME dipole excited by two simple Γ-shaped strips is presented in [16], where wide impedance bandwidth and good isolation between ports are achieved. A wideband dual-LPME dipole antenna using differentially-driven scheme has been reported in [17] for realizing high port isolation and low cross-polarization levels. Moreover, in [18], a broadband dual-polarized ME dipole antenna based on dielectric loading is reported, and broadband dual-polarized ME dipoles with simple feeding and meta-columns loading have been proposed in [19–21], which further demonstrate huge potential application values of ME dipole in multiple polarization diversity.

Unfortunately, most of these works mentioned above have cumbersome structures and only operate at linear polarization states. Therefore, it is still very challenging to design a wideband dual-CP ME dipole using simple and easy-to-implement structures. A wideband dual-CP ME dipole antenna using novel crossed feeding structures is proposed in this work. The crossed feeding structures contain four orthogonal excitation ports and four 3-stage printed impedance transitions, each of which is folded as a Γ-shaped branch for exciting ME dipole radiation structures. Two wideband feeding networks based on a wideband Wilkinson power divider and coupled-line phase shifter are utilized to provide demanded two-way output signals for generating wideband dual-CP radiation. Measured results show that the proposed antenna exhibits a wide overlapped operation bandwidth of 53.2%, which covers most application frequency bands in S-band. Detailed design procedures are given as follows.

2. ANTENNA DESIGN

2.1. Antenna Configuration

Configurations of the proposed ME dipole antenna are depicted in Fig. 1, from which one can see that the proposed antenna consists of our same radiation structures, novel crossed feeding structures, two

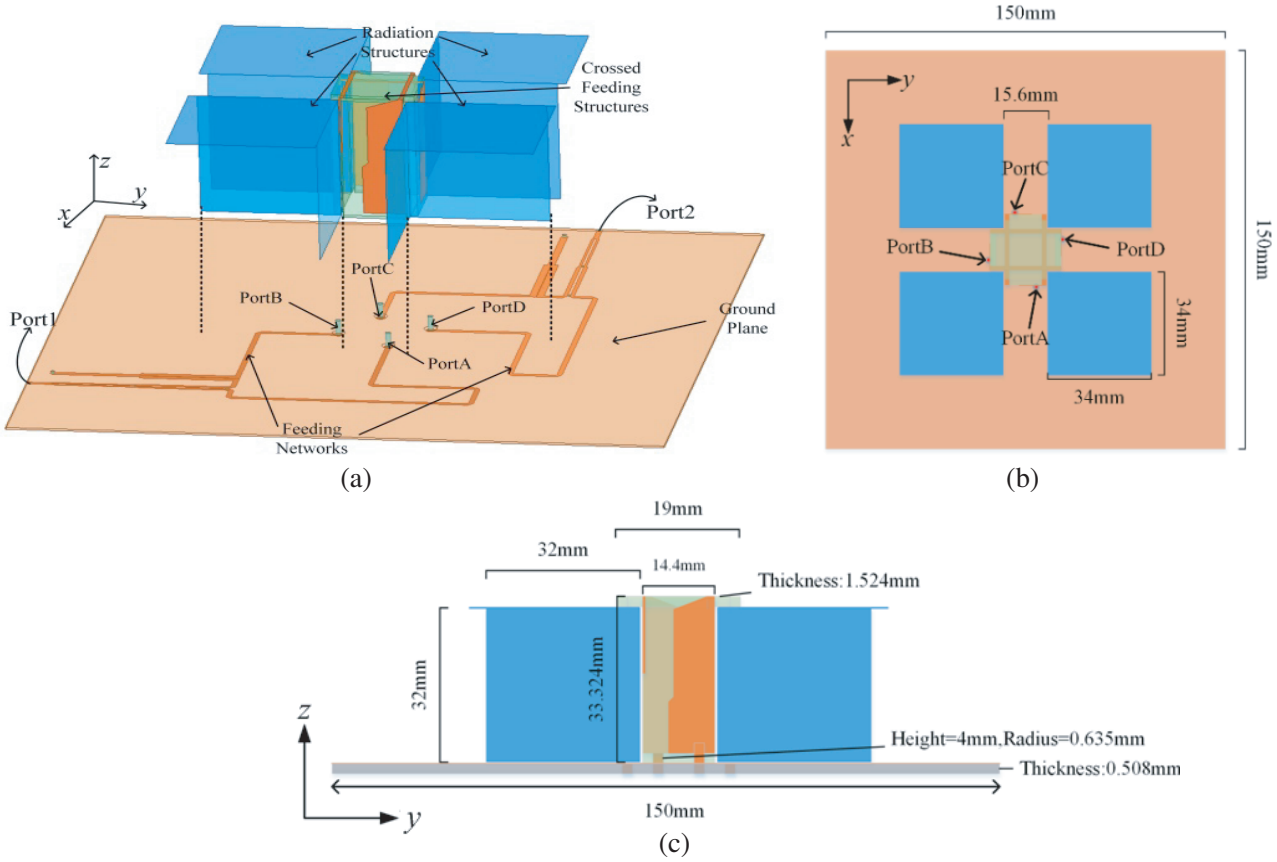

Figure 1. Geometry of the proposed antenna: (a) 3D exploded view; (b) Top view; (c) Side view.

feeding networks, and a square ground plane. The radiation structure functions as a ME dipole, and four horizontal patches constitute an electric dipole, while the aperture between the vertically oriented shorted patches realizes the magnetic dipole. The radiation patterns of electric dipole and magnetic dipole are just complementary in E-plane and H-plane, and the fields will be superimposed in phase in one direction and cancel reverse phase in the other direction, resulting in producing a directional radiation beam. As shown, a novel feeding schematic with four orthogonal excitation ports (Port A, Port B, Port C, and Port D) based on crossed Γ-shaped folded branches has been designed to achieve wideband characteristics.

Detailed sizes of the novel crossed feeding structures are shown on the right side of Fig. 2 with unfolded view. From Fig. 2, one can see that each of the feeding structures has three stages with different widths and lengths. For the purpose of realizing low profile, the feeding structure can be folded as a Γ-shaped branch, which works as a 3-stage impedance matching transmission line which provides wideband impedance matching between the ME dipole radiators and excitation ports. The RF signals are coupled to the radiation structures through the Γ-shaped branches. The feeding structures are not in direct contact with the radiation structures, and the coupling distance affects the radiation fields little. In order to enhance the isolation between excitation ports and for easy fabrication, the Γ-shaped branches are printed on the substrates with a thickness of 1.524 mm. The second stages of each Γ-shaped branch are especially printed on the different sides of the top substrate, which reduces the coupling of the electromagnetic wave from the excitation ports on the opposite side. Each of the Γ-shaped branches is connected to a feeding probe which is a metallic cylinder connecting to the feeding network. All of the feeding structures can be printed on the substrates by using PCB technique, which greatly simplify the processing complexity and improve the fabrication accuracy.

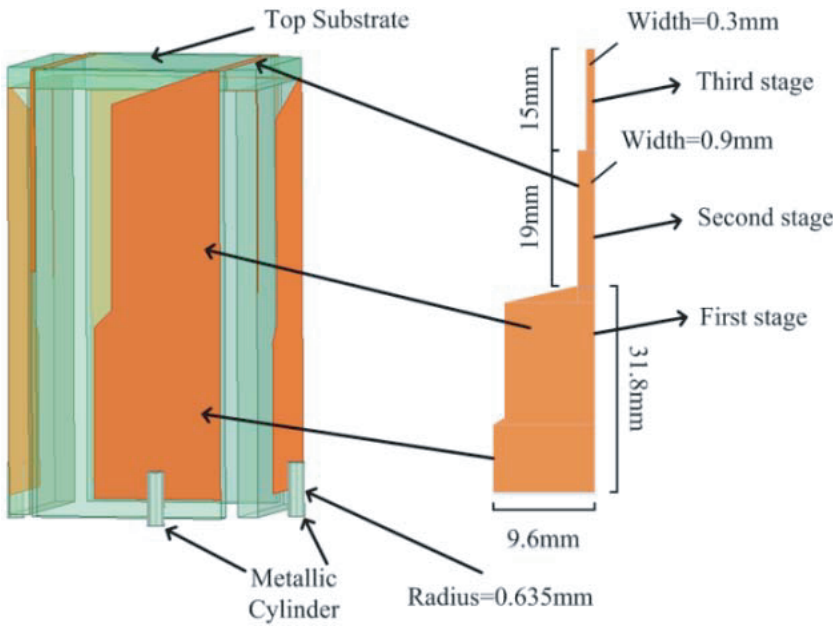

Figure 2. Geometry of crossed feeding structures.

The ground plane is printed on the top layer of the lower substrate with a thickness of 0.508 mm, while two wideband feeding networks with two input ports (Port 1 and Port 2) are printed on the bottom layer of the substrate to provide signals with quadrature-phase for generating dual-CP. A wideband Wilkinson power-divider [22] and a wideband 90° coupled-line phase shifter [23] are utilized to provide the desired equal-amplitude and quadrature-phase in a wide frequency band, and their circuit models can be analyzed by using the rigorous odd- and even-mode theory. When signals are input from Port 1, Port A and Port B are excited with equal-amplitude and quadrature-phase simultaneously, contributing to forming right-hand circular polarization (RHCP) waves. On the other hand, when Port 2 is excited,

signals are transmitted to Port C and Port D for generating left-hand circular polarization (LHCP) waves.

In this design, Rogers 4003C is used as the substrates, with a relative permittivity of 3.38 and a loss tangent of 0.0027. The other metal parts are all materials of copper with a thickness of 0.3 mm. The radius of the four metallic cylinders is 0.635 mm, and the height of them is 4 mm.

2.2. Wideband Circularly Polarized ME Dipole Design

In order to realize the performance of wideband circular polarization, a wideband feeding network has been designed to feed the crossed Γ-shaped branches. Its geometry and detailed sizes are depicted in Fig. 3. When signals are fed into Port 1, they are divided into two-way outputs with equal amplitude after passing through a two-stage wideband Wilkinson power divider. Then, one way of the divided signals passes through a 90° coupled-line phase shifter, which generates a 90° phase difference between Ports A and B. Both of the divided signals will be transmitted to the crossed Γ-shaped feeding structures

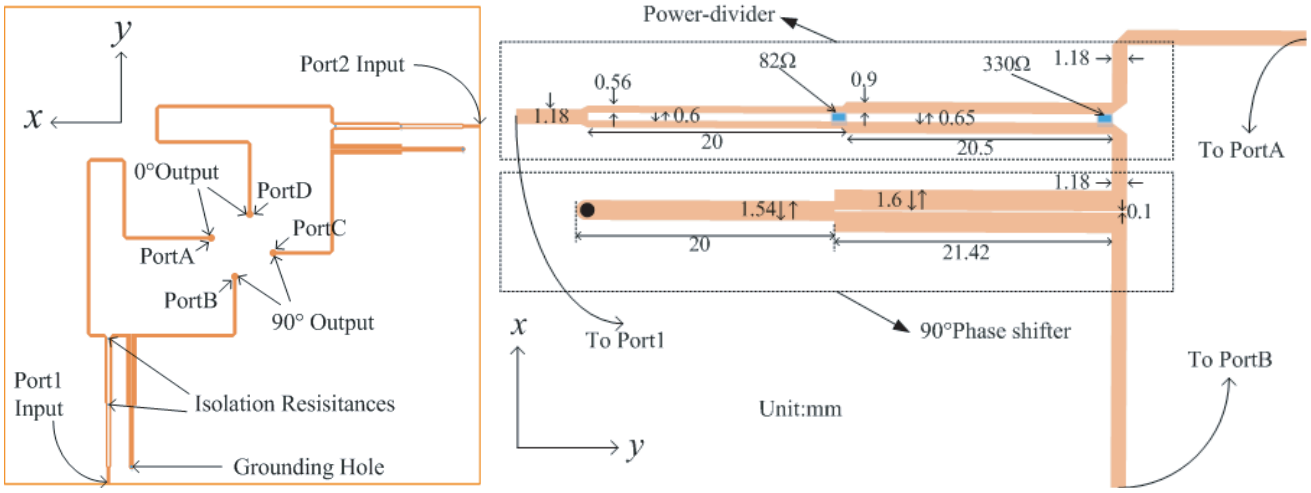

Figure 3. Geometry of the wideband feeding network: (a) The overview; (b) Detailed sizes.

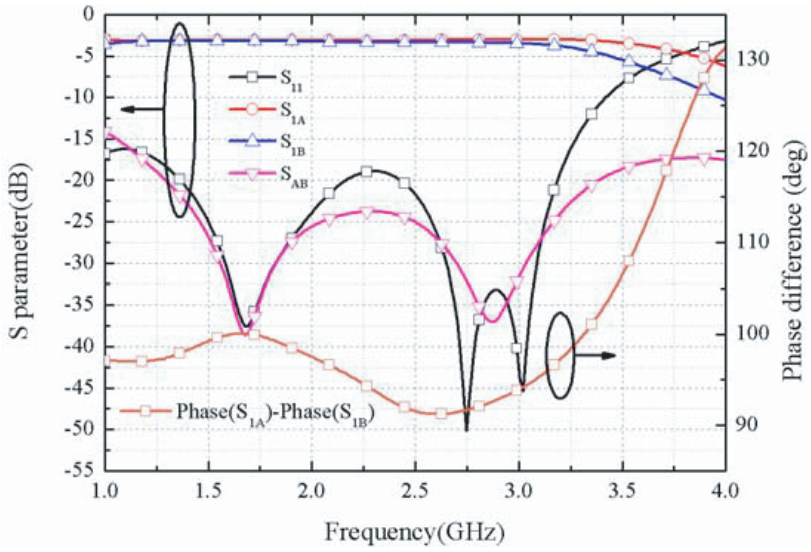

Figure 4. Simulated scattering parameter responses of the proposed feeding network.

through the metallic cylinders. The proposed antenna works at RHCP radiation mode by exciting Port 1, while it works at LHCP radiation mode when Port 2 is used. The simulated scattering parameter responses of the wideband feeding network are given in Fig. 4. As shown, the feeding network has an operation bandwidth of 88.8% from 1.06 to 3.28 GHz (defined by 10-dB return loss, 15-dB isolation, and 1-dB insertion loss).

For the purpose of further clarifying the operating mechanism of the proposed dual-CP ME dipole, the surface currents distribution at different times of $t = 0$, $T/4$, $T/2$, and $3T/4$ are shown in Fig. 5, where T is the signal oscillation period at the center frequency 2.5 GHz. Considering that the radiation structures of the proposed antenna are symmetric, for concise, only the currents distributions of RHCP (exciting by Port 1) are presented. It can be seen that at different times the equivalent total currents (represented by the black arrows) show a trend of anti-clockwise rotation, which facilitates an RHCP radiation wave.

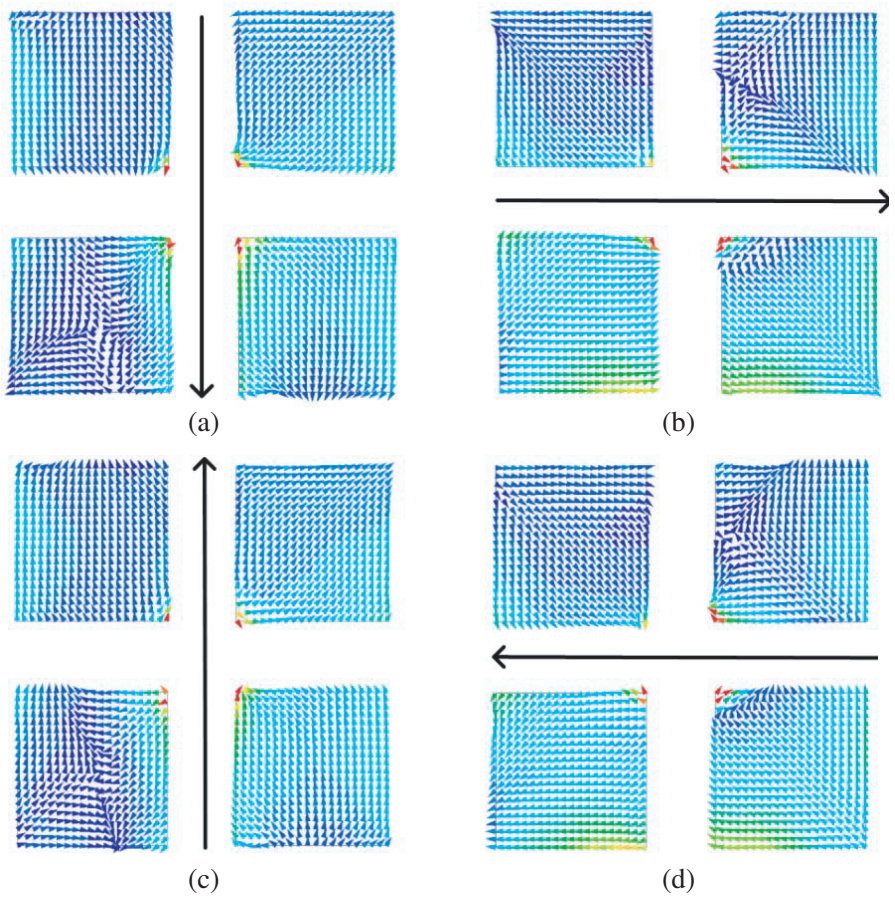

Figure 5. Surface currents distribution of the proposed ME dipole on the radiation patches at 2.5 GHz: (a) $t = 0$; (b) $t = T/4$; (c) $t = T/2$; (d) $t = 3T/4$.

3. SIMULATED AND MEASURED RESULTS

The antenna was simulated and optimized by using a high frequency structure simulator. The optimization goal is to maximize the impedance and axial ratio operation bandwidth on the basis of maintaining the port isolation less than -10 dB. The measurements on S parameters, gain, and radiation patterns are conducted with a vector network analyzer and a near-field measurement system. The photographs of the fabricated antenna and test environment are depicted in Fig. 6.

The measured and simulated S parameters of the proposed antenna are given in Fig. 7, from which one can see that the simulated and measured impedance bandwidths of Port 1 are 62% from 1.63 GHz

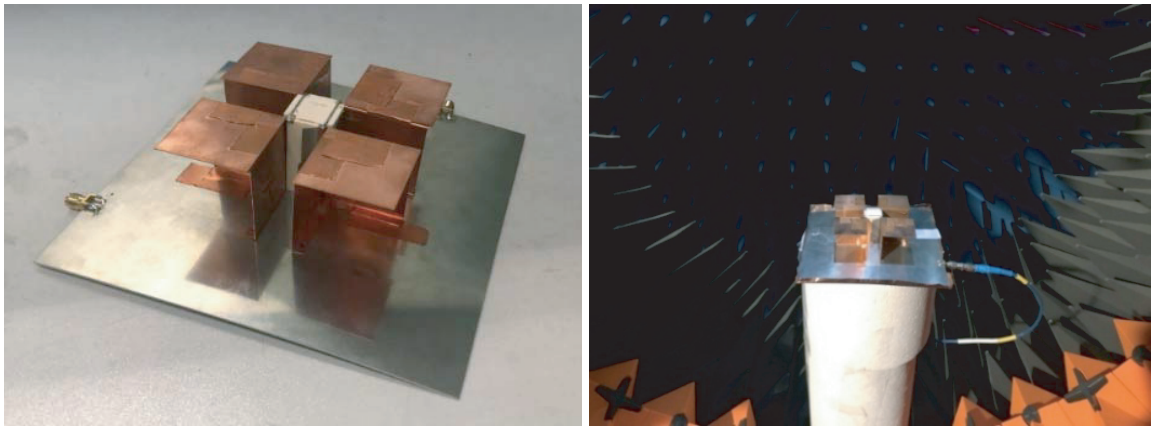

(a) (b)

Figure 6. Photographs of the antenna prototype: (a) The fabricated prototype; (b) The proposed antenna in the testing system.

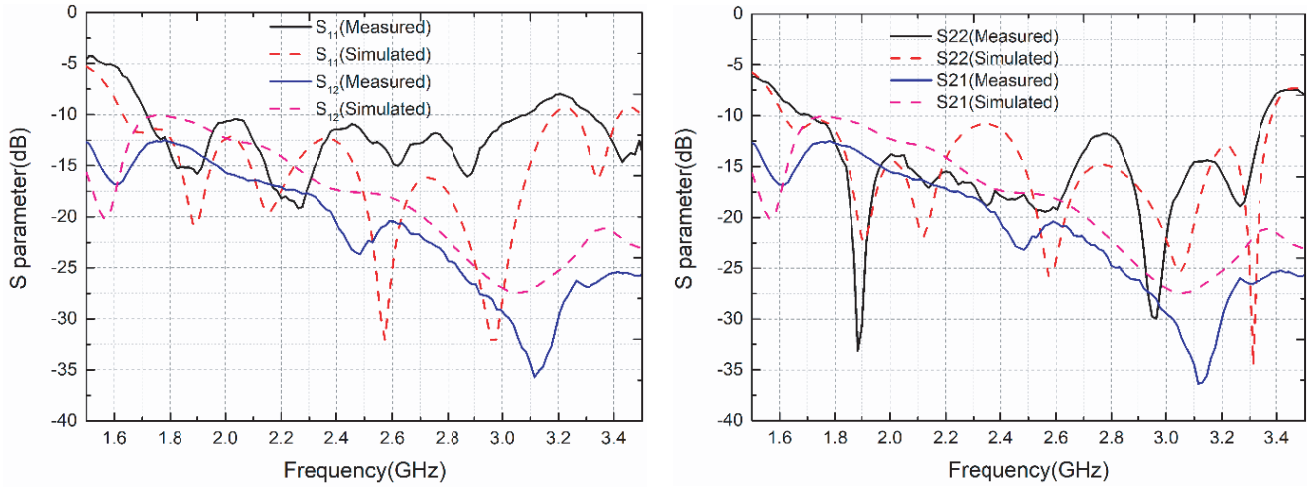

(a) (b)

Figure 7. Simulated and measured S parameters of the proposed antenna: (a) Simulated and measured S parameters of Port 1; (b) Simulated and measured S parameters of Port 2.

to 3.18 GHz and 55.6% from 1.71 GHz to 3.11 GHz. As for Port 2, they are 70.8% from 1.61 GHz to 3.38 GHz and 66.4% from 1.70 GHz to 3.36 GHz, in which the simulated and measured isolations are both better than −12 dB.

The simulated and measured AR and gain curves at two working modes are shown in Fig. 8. As demonstrated, the simulated AR bandwidths of the RHCP and LHCP are 60.8% from 1.5 GHz to 3.02 GHz and 72.8% from 1.5 GHz to 3.32 GHz, while the measured ones are 54% from 1.6 GHz to 2.95 GHz and 66% from 1.6 GHz to 3.25 GHz. Besides, measured and simulated peak gain values of RHCP are 6.6 dBic and 7 dBic (both at 2.6 GHz), while they are 6.6 dBic (at 2.4 GHz) and 6.6 dBic (at 2.54 GHz) for LHCP. As such, the available operation bandwidth is 53.2% for RHCP from 1.71 GHz to 2.95 GHz and 62% for LHCP from 1.7 GHz to 3.25 GHz, respectively. The whole size of the proposed antenna is about $0.85\lambda \times 0.85\lambda \times 0.18\lambda$, where λ is the vacuum wavelength at the low frequency 1.71 GHz.

The operating frequency bands for Port 1 and Port 2 are slightly different. This is probably due to the small difference in dimensions and locations of the printed Γ-shaped branches and the slight asymmetry between the feeding networks. The discrepancies between measured and simulated results

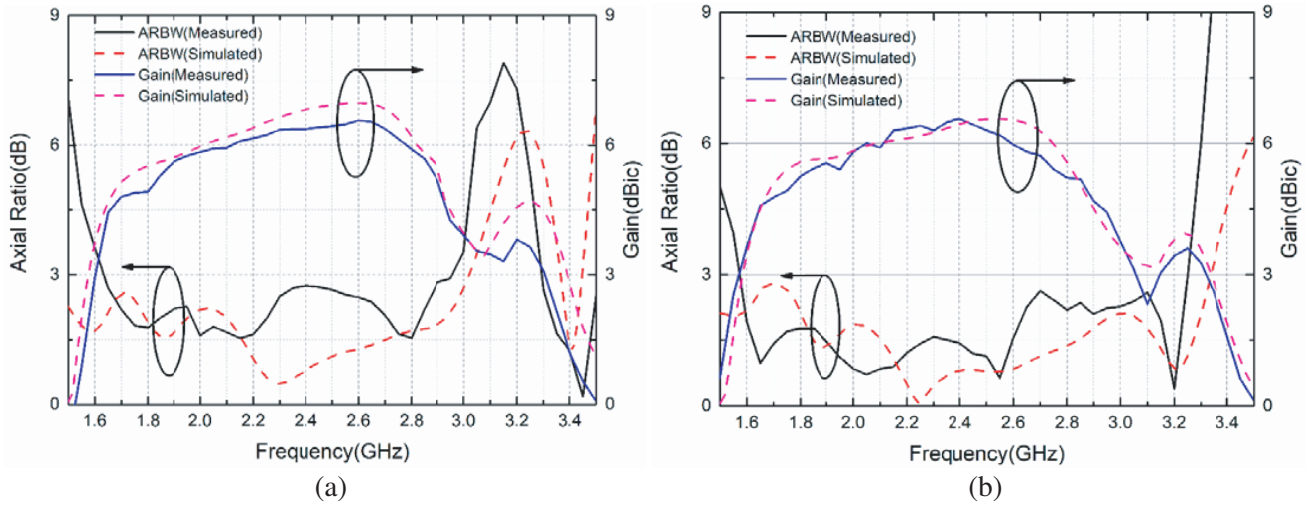

Figure 8. Simulated and measured AR and gain curves of the proposed antenna: (a) Port 1 excitation (RHCP mode); (b) Port 2 excitation (LHCP mode).

are likely caused by slight distortions of the mechanical copper parts, assembling errors, and installing and measuring tolerances.

The radiation patterns at a low frequency 2 GHz and a high frequency 2.8 GHz in two principal planes under different polarization states are depicted in Fig. 9. It can be seen from this figure that the proposed antenna exhibits stable unidirectional radiation patterns for two polarization modes in both observed planes.

Comparisons between our design and other typical ME dipole antennas reported in the recent literatures [15, 18–20, 24, 25] are given in Table 1. The designs present in [15, 18] are only operated in dual-LP modes. As for the antennas in [19, 24], they have higher peak gains and medium operation bandwidth, but they suffer from large sizes. Ref. [20] gives a dual-CP design with wideband and a more compact size, whereas its radiation gain is relatively low, and the fabrication process is relatively complex. By comparison, the proposed dual-CP antenna exhibits simpler radiation structures, and it is easier to be fabricated through using PCB technique. Besides, our design has the widest effective overlapped bandwidth with a medium size and moderate gain, which makes it have an enormous potential in several application scenarios, including radio determination satellite service (RDSS) (2.483–2.5 GHz), WLANs (2.400–2.484 GHz), RFID (2.446–2.454 GHz), and 2.5 GHz WiMAX, etc.

Table 1. Comparisons of the proposed ME dipole with other related antennas.

Ref.	Polarization States	Size (λ^3)	Frequency (GHz)	Effective Bandwidth (%)	Peak Gain (dBi)
15	2 LP, 1 CP	$0.87 \times 0.65 \times 0.18$	1.74–2.45	33.9	8.2
18	2 LP	$0.71 \times 0.71 \times 0.13$	1.65–2.12	24.9	8.2
19	2 CP	$1.1 \times 1.1 \times 0.26$	2.23–3.35	40.1	10
20	2 CP	$0.66 \times 0.66 \times 0.16$	3.2–5.4	51	6
24	2 CP	$0.91 \times 0.91 \times 0.25$	5.07–5.95	16	8.2
25	1 CP	$0.67 \times 0.67 \times 0.17$	4.98–6.31	23.5	7.5
Prop.	2 CP	$0.85 \times 0.85 \times 0.18$	1.71–2.95	53.2	6.6

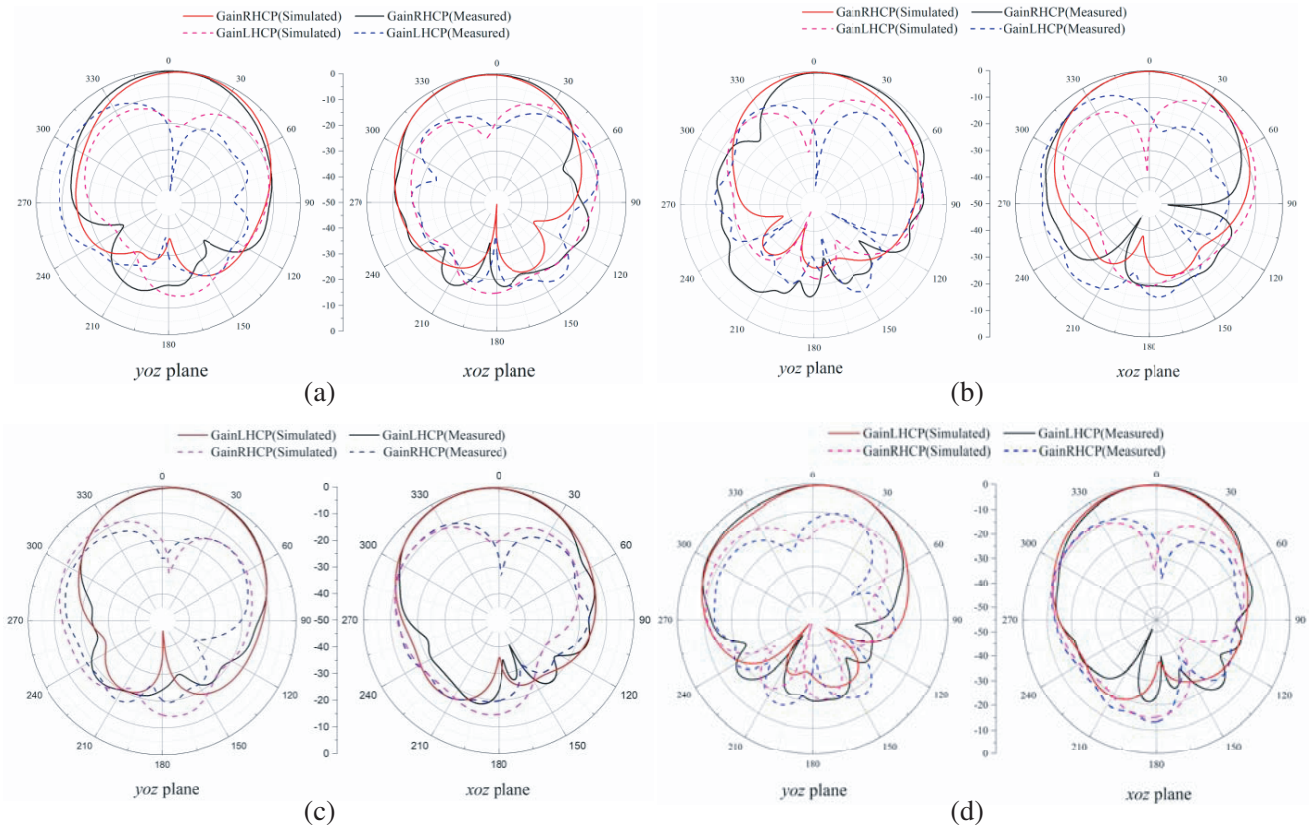

Figure 9. Simulated and measured radiation patterns of the proposed dual-CPME dipole: (a) RHCP mode with Port 1 excitation at 2 GHz; (b) RHCP mode with Port 1 excitation at 2.8 GHz; (c) LHCP mode with Port 2 excitation at 2 GHz; (d) LHCP mode with Port 2 excitation at 2.8 GHz.

4. CONCLUSION

A wideband dual circularly polarized ME dipole antenna based on novel crossed feeding structures is presented in this paper. The crossed feeding structures consists of four 3-step impedance transformation transitions which are folded as Γ-shaped branches and can be easily printed on substrates for simplifying the manufacturing process. By utilizing two wideband quadrature-phase feeding networks, desired wideband characteristics with dual-CP operation are achieved. Measured results show that the proposed antenna has stable dual-CP radiation patterns within the operation band. The overlapped bandwidth is 53.2% for RHCP from 1.71 GHz to 2.95 GHz and 62% for LHCP from 1.7 GHz to 3.25 GHz, respectively. Compared with other typical designs, the proposed antenna shows wider effective overlapped bandwidth with a medium size and moderate gain making it a suitable candidate to be used in some real wireless systems, such as radio determination satellite service (RDSS), WLANs, RFID, and WiMAX.

ACKNOWLEDGMENT

This work was supported in part by the National Natural Science Foundation of China, Grant/Award Number: 61871083, 61721001 and 61601103.

REFERENCES

1. Ma, S. and J. Row, "Design of single-feed dual-frequency patch antenna for GPS and WLAN applications," *IEEE Trans. Antennas Propag.*, Vol. 59, No. 9, 3433–3436, 2011.

2. Ta, S. X., I. Park, and R. W. Ziolkowski, "Circularly polarized crossed dipole on an HIS for 2.4/5.2/5.8-GHz WLAN applications," *IEEE Antennas Wirel. Propag. Lett.*, Vol. 12, 1464–1467, 2013.
3. Sim, C., Y. Hsu, and G. Yang, "Slits loaded circularly polarized universal UHF RFID reader antenna," *IEEE Antennas Wirel. Propag. Lett.*, Vol. 14, 827–830, 2015.
4. Arnieri, E., L. Boccia, G. Amendola, and G. D. Massa, "Acompact high gain antenna for small satellite application," *IEEE Trans. Antennas Propag.*, Vol. 55, No. 2, 277–282, 2007.
5. Le, T. T. and H. H. Tran, "Dual-band dual-sense circularly polarized antenna based on crossed dipole structure for WLAN/WiMAX applications," *Int. J. RF Microw. Comput. Eng.*, Vol. 29, No. 10, e21866, 2019.
6. Chaudhuri, S., R. S. Kshetrimayum, and R. K. Sonkar, "High inter-port isolation dual circularly polarized slot antenna with interdigital capacitor," *Int. J. RF Microw. Comput. Eng.*, Vol. 29, No. 10, e21903, 2019.
7. Saini, R. K., P. S. Bakariya, and P. Kumar, "Coplanar waveguide fed dual-band dual-sense circular polarized square slot antenna," *Int. J. RF Microw. Comput. Eng.*, Vol. 28, No. 9, e21503, 2018.
8. Xu, L., W. J. Lu, C. Y. Yuan, and L. Zhu, "Dual circularly polarized loop antenna using a pair of resonant even-modes," *Int. J. RF Microw. Comput. Eng.*, Vol. 29, No. 6, e21703, 2019.
9. Luk, K. and H. Wong, "A new wideband unidirectional antenna element," *Int. J. Microw. Opt. Technol.*, Vol. 1, No. 1, 35–44, 2006.
10. Yang, K. W., F. S. Zhang, C. Li, Z. H. Zhang, and F. Zhang, "A wideband aperture coupled magneto-electric dipole with high gain stability," *Int. J. RF Microw. Comput. Eng.*, Vol. 30, No. 7, e22197, 2020.
11. Yan, S., P. J. Soh, and G. A. E. Vandenbosch, "Wearable dual-band magneto-electric dipole antenna for WBAN/WLAN applications," *IEEE Trans. Antennas Propag.*, Vol. 63, No. 9, 4165–4169, 2015.
12. Kang, K., Y. Shi, and C. H. Liang, "Substrate integrated magneto-electric dipole for UWB application," *IEEE Antennas Wirel. Propag. Lett.*, Vol. 16, 948–951, 2017.
13. Ding, C. and K. Luk, "Low-profile magneto-electric dipole antenna," *IEEE Antennas Wirel. Propag. Lett.*, Vol. 15, 1642–1644, 2016.
14. Wu, F. and K. M. Luk, "A reconfigurable magneto-electric dipole antenna using bent cross-dipole feed for polarization diversity," *IEEE Antennas Wirel. Propag. Lett.*, Vol. 16, 412–415, 2017.
15. Shi, Y., Y. Cai, X. F. Zhang, and K. Kang, "A simple tri-polarization reconfigurable magneto-electric dipole antenna," *IEEE Antennas Wirel. Propag. Lett.*, Vol. 17, No. 2, 291–294, 2018.
16. Wu, B. Q. and K. Luk, "A broadband dual-polarized magneto-electric dipole antenna with simple feeds," *IEEE Antennas Wirel. Propag. Lett.*, Vol. 8, 60–63, 2009.
17. Xue, Q., S. W. Liao, and J. H. Xu, "A differentially-driven dual-polarized magneto-electric dipole antenna," *IEEE Trans. Antennas Propag.*, Vol. 61, No. 1, 425–430, 2013.
18. Siu, L., H. Wong, and K. M. Luk, "A dual-polarized magneto-electric dipole with dielectric loading," *IEEE Trans. Antennas Propag.*, Vol. 57, No. 3, 616–623, 2009.
19. Chen, W., Z. Yu, J. Zhai, and J. Zhou, "Developing wideband dual-circularly polarized antenna with simple feeds using magnetoelectric dipoles," *IEEE Antennas Wirel. Propag. Lett.*, Vol. 19, No. 6, 1037–1041, 2020.
20. Feng, B., L. Li, K. L. Chung, and Y. Li, "Wideband widebeam dual circularly polarized magnetoelectric dipole antenna/array with meta-columns loading for 5G and beyond," *IEEE Trans. Antennas Propag.*, Vol. 69, No. 1, 219–228, 2021.
21. Tianang, E. G., M. A. Elmansouri, L. Boskovic, and D. S. Filipovic, "Design of a dual-circularly polarized X-band active phased array based on a balanced-diplexer," *2019 IEEE International Symposium on Phased Array System & Technology (PAST)*, 1–5, 2019.
22. Wu, Y., Y. Liu, and Q. Xue, "An analytical approach for a novel coupled-line dual-band Wilkinson power divider," *IEEE Trans. Microw. Theory Tech.*, Vol. 59, No. 2, 286–294, 2011.
23. Liu, Q., H. Liu, and Y. Liu, "Compact ultra-wideband 90° phase shifter using short-circuited stub and weak coupled line," *Electron. Lett.*, Vol. 50, No. 20, 1454–1456, 2014.

24. Ge, L., X. Yang, D. Zhang, M. Li, and H. Wong, "Polarization-reconfigurable magnetoelectric dipole antenna for 5G Wi-Fi," *IEEE Antennas Wirel. Propag. Lett.*, Vol. 16, 1504–1507, 2017.
25. Sun, K., D. Yang, and S. Liu, "A wideband hybrid feeding circularly polarized magneto-electric dipole antenna for 5G Wi-Fi," *Microw. Opt. Technol. Lett.*, Vol. 60, No. 8, 1837–1842, 2018.